Korean J Physiol Pharmacol
Vol 17: 189−195, June, 2013
http://dx.doi.org/10.4196/kjpp.2013.17.3.189

Altered APP Carboxyl-Terminal Processing Under Ferrous Iron Treatment in PC12 Cells

Chi Hyun Kim, and Yeong-Min Yoo

Department of Biomedical Engineering, College of Health Science, Yonsei University, Wonju 220-710, Korea

Amyloid-β peptide (Aβ), generated by proteolytic cleavage of the amyloid precursor protein (APP), plays a pivotal role in the pathogenesis of Alzheimer's disease (AD). The key step in the generation of Aβ is cleavage of APP by beta-site APP-cleaving enzyme 1 (BACE1). Levels of BACE1 are increased in vulnerable regions of the AD brain, but the underlying mechanism is unknown. In the present study, we reported the effects of ferrous ions at subtoxic concentrations on the mRNA levels of *BACE1* and a-disintegrin-and-metalloproteinase 10 (*ADAM10*) in PC12 cells and the cell responses to ferrous ions. The cell survival in PC12 cells significantly decreased with 0 to 0.3 mM $FeCl_2$, with 0.6 mM $FeCl_2$ treatment resulting in significant reductions by about 75%. 4,6-diamidino-2-phenylindole (DAPI) staining showed that the nuclei appeared fragmented in 0.2 and 0.3 mM $FeCl_2$. APP-α-carboxyl terminal fragment (APP-α-CTF) associations with ADAM10 and APP-β-CTF with BACE1 were increased. Levels of *ADAM10* and *BACE1* mRNA increased in response to the concentrations of 0.25 mM, respectively. In addition, p-ERK and p-Bad (S112, S155) expressions were increased, suggesting that APP-CTF formation is related to *ADAM10/BACE1* expression. Levels of Bcl-2 protein were increased, but significant changes were not observed in the expression of Bax. These data suggest that ion-induced enhanced expression of AMDA10/BACE1 could be one of the causes for APP-α/β-CTF activation.

Key Words: ADAM10, APP-α/β-CTF, APP processing, BACE1, Ferrous iron, p-ERK

INTRODUCTION

Alzheimer's disease (AD) is the most prevalent neurodegenerative disease worldwide. Its pathological features include synaptic degeneration, senile plaques and neurofibrillary tangles, which eventually lead to neuronal loss [1]. The major components of senile plaque are amyloid-β peptide (Aβ), which are derived by proteolytic cleavage of amyloid precursor protein (APP), a type I membrane spanning protein. Two enzymes, beta-site APP-cleaving enzyme 1 (BACE1; originally referred to as BACE) and BACE2, are involved in Aβ production. BACE1 is mainly responsible for β-cleavage of APP *in vivo*, and overexpression of BACE1 increases the production of Aβ in vitro. Therefore, BACE1 is considered the pivotal component in Aβ production [2]. Since less than 10% of total AD cases are associated with genetic factors [3], it is extremely important to investigate how environmental factors contribute to the pathogenesis of this disease.

Although the cause or causes of AD are not yet known, most experts agree that AD probably develops as a result of multiple factors rather than a single cause. The greatest risk factor for AD is advancing age [4]. The risk of AD dramatically increases in individuals beyond the age of 70, and it is predicted that the incidence of AD will increase three-fold within the next 50 years [2]. Recent findings suggest that age-related increases in oxidative stress account for aspects of AD [5]. Some evidence demonstrates that oxidative stress is an early event in AD, occurring prior to cytopathology, and therefore may play a key pathogenic role in the disease [6]. It has been reported that iron can accelerate the production of Aβ and is found in high concentrations in the amyloid plaque [7].

The influence of metal ions on AD pathogenesis is becoming evident. Although essential for cell function, increased tissue iron can promote tissue oxidative damage to the brain, which is especially vulnerable [8,9]. In the human brain, iron levels increase with age [10,11], and iron contributes to the development of proteinopathies (abnormal deposits of proteins) associated with several prevalent neurodegenerative diseases such as AD, Parkinson's disease (PD), and Dementia with Lewy Bodies (DLB) [8,12]. Iron

Received January 14, 2013, Revised April 12, 2013,
Accepted April 12, 2013

Corresponding to: Yeong-Min Yoo, Department of Biomedical Engineering, College of Health Science, Yonsei University, 162, Ilsan-dong, Wonju 220-710, Korea. (Tel) 82-33-760-2898, (Fax) 82-33-760-2898, (E-mail) yooym@yonsei.ac.kr

ABBREVIATIONS: Aβ, amyloid-β peptide; APP, amyloid precursor protein; AD, Alzheimer's disease; BACE1, APP-cleaving enzyme 1; APP-α-CTF, APP-α-carboxyl terminal fragment; APP-β-CTF, APP-β-carboxyl terminal fragment; ADAM10, a-disintegrin-and-metalloproteinase 10; ERK, extracellular signal-regulated kinase.

levels are abnormally elevated in these age-related neurodegenerative diseases, suggesting that increased iron levels may contribute to their age risk-factor as well as impacting the age at onset especially in males [13]. Although a few studies focused on the effects of metal ions on the transcription of APP, their effects on BACE1, the other pivotal component of Aβ production, are still not well understood.

The potential signal transduction pathway involved in the pathology of AD may be the activation of the MAPKs. MAPKs are classified into different subfamilies, and among them, the best known are the extracellular signal regulated kinase (ERK), the c-Jun N-terminal kinase (JNK) and p38 [14]. The ERK-signal pathway results in phosphorylation of Bad at serine-112 (S1112) and -155 (S155) [15]. Increased Bad phosphorylation reduces its translocation to mitochondria, limits the release of mitochondrial cytochrome c [16] and apoptosis-inducing factor, and increases the resistance to apoptosis. It has been reported that prolonged ERK activation is accompanied by the proapoptotic effect of ERK [17], whereas transient activation of ERK protects cells from death [18].

Bcl-2 families are well-characterized regulators of apoptosis, consisting of three distinct subfamilies. The Bcl-2 subfamily contains antiapoptotic proteins, such as Bcl-2 and Bcl-XL, which reduce the release of cytochrome c [19,20]. The Bax subfamily contains proapoptotic proteins such as Bax and Bak, which induce the release of cytochrome c [21]. Furthermore, the ratio of proapoptotic and antiapoptotic Bcl-2 proteins may be a pivotal cue to release cytochrome c from mitochondria.

Oxidative stress induces *BACE1* transcription [22], thereby promoting the production of Aβ [23]. Aβ has iron chelating sites [24], thus protecting the cells from oxidative stress. Therefore, in the present study, we investigated the mRNA levels of *BACE1/ADAM10* and altered APP carboxyl-terminal processing under ferrous iron treatment in PC12 cells.

METHODS

PC12 cell culture

The PC12 cells were cultured in Dulbecco's Modified Eagle's Medium (DMEM; Gibco, NY, USA) supplemented with 10% fetal bovine serum (FBS; Hyclone Laboratories, Logan, UT, USA), 5 μg/ml plasmocin, 100 U/ml penicillin, and 100 μg/ml. For induction of oxidative condition, PC12 cells were treated with $FeCl_2$ (0.05, 0.1, 0.15, 0.2, 0.25, 0.3, and 0.6 mM) and then incubated at 37°C with 95% air and 5% CO_2 for 30 hr.

Cell survival assay

A Cell Counting Kit-8 (CCK-8; Tokyo, Japan) was used in this study. One hundred microliters of cell suspension without FBS was dispensed into a 96-well plate. $FeCl_2$ (0.05, 0.1, 0.15, 0.2, 0.25, 0.3, and 0.6 mM) was added to the plate wells, respectively. The plates were incubated at 37°C with 95% air/5% CO_2 for 30 hr. Then, 10 μl of CCK-8 solution was added to each well of the plate and incubated for 1 hr. Absorbance was measured with a microplate reader (Molecular Devices, Sunnyvale, CA, USA) at 450 nm.

DAPI staining

PC12 cells were washed extensively with serum-free DMEM and replated onto new 6-well plates. Cells were fixed in 4% paraformaldehyde buffered with 0.1 M phosphate (pH 7.3) for 30 min and then washed with phosphate buffered saline (PBS). The cells were permeabilized with 0.3% Triton X-100 for 20 min, washed with PBS, and then stained with 4,6-diamidino-2-phenylindole (DAPI, Santa Cruz Biotechnology, CA, USA) for 10 min. Cells were observed by fluorescence microscopy (Olympus IX71, Japan) at a peak excitation wavelength of 340 nm.

RNA extraction and quantitative real-time PCR

Total RNA was extracted using Trizol reagent (Invitrogen Co., Carlsbad, CA, USA) according to the manufacturer's instructions, and the concentration of total RNA was determined by measuring the absorbance at 260 nm. A first strand complementary DNA (cDNA) was prepared by subjecting total RNA (1 μg) to reverse transcription using moloney murine leukemia virus (MMLV) reverse transcriptase (iNtRON Bio, Sungnam, Kyunggi, Korea) and random primers (9-mers; TaKaRa Bio Inc, Otsu, Shiga, Japan). Each cDNA template (2 μl) was analyzed in triplicate by addition of 10 μl of 2× SYBR® Premix Ex Taq™ (TaKaRa Bio. Inc., Otsu, Shiga, Japan) along with 10 pmol of each primer. Amplification was conducted using a 7,300 Real-Time PCR System (Applied Biosystems, Foster, CA, USA) and the following parameters: denaturation at 95°C for 5 minutes; 40 cycles of denaturation at 95°C for 30 seconds; and annealing and extension at 63°C for 30 seconds and 72°C for 45 seconds, respectively. The sequences of the oligonucleotides used for amplification were as follows: *ADAM10* forward, 5'-AGCAACATCTGGGGACAAAC-3'; *ADAM10* reverse, 5'-TTGCACTGGTCACTGTAGCC-3'; *BACE1* forward, 5'-TCGCTGTCTACAGTCATCC-3'; *BACE1* reverse, 5'-AACAAACGGACCTTCCACTG-3'; *β-actin* forward, 5'-AGCCATGTACGTAGCCATCC-3'; *β-actin* reverse, 5'-TTTGATGTCACGCACGATTT-3'. The relative expression levels of *ADAM10* and *BACE1* (normalized to that of *β-actin*) for each sample were determined using RQ software (Applied Biosystems). All real-time PCR experiments were repeated twice.

Western blot analysis

Cells were harvested, washed twice with ice-cold PBS, and then resuspended in 20 mM Tris-HCl buffer (pH 7.4) containing protease inhibitors (0.1 mM phenylmethyl-sulfonyl fluoride, 5 μg/ml aprotinin, 5 μg/ml pepstatin A, and 1 μg/ml chymostatin) and phosphatase inhibitors (5 mM Na_3VO_4, 5 mM NaF). Whole cell lysate was prepared using 20 strokes of a Dounce homogenizer, followed by centrifugation at 13,000×g for 20 min at 4°C. Protein concentration was determined using the BCA assay (Sigma, St Louis, MO, USA). Proteins (50 μg) were separated by 12% sodium dodecyl sulfate-polyacrylamide gel electrophoresis (SDS-PAGE) and then transferred onto a polyvinylidene difluoride (PVDF) membrane. The membrane was incubated with antibodies directed against the following proteins, as indicated: phosphorylated (p)-ERK (1 : 1,000), ERK (1 : 1,000) (Transduction Laboratories, Lexington, KY, USA); p-Bad (S112, 136, 155) (Cell Signaling Technology, Beverly, MA, USA) (1 : 1,000); Bad, Bax, and Bcl-2 (Santa Cruz

Biotechnology, CA, USA) (1 : 500); GAPDH (1 : 1,000) (Assay Designs, MI, USA); anti-APP (Santa Cruz Biotechnology, CA, USA) (1 : 500). Immunoreactive proteins were visualized by exposure to X-ray film. The protein bands were quantified by image-scanning, and optical density was measured using computer software (NIH Image software 1.52), after the data was corrected by background subtraction and normalized to glyceraldehyde 3-phosphate dehydrogenase (GAPDH), an internal control.

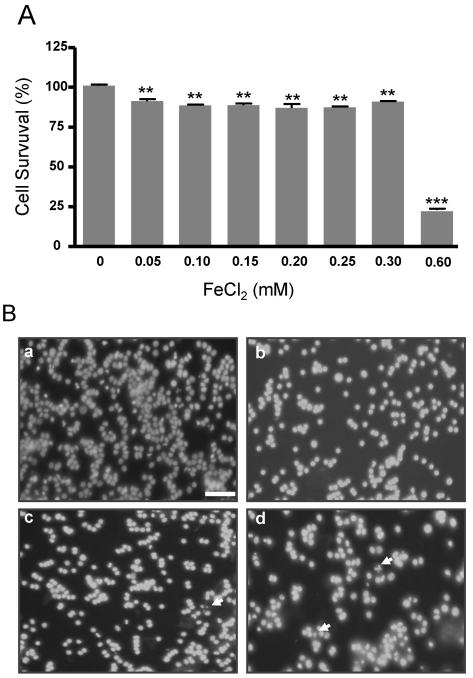

Fig. 1. Cell viability under $FeCl_2$ treatment in PC12 cells. PC12 cells were incubated in DMEM containing 10% FBS and increasing concentrations of $FeCl_2$ from 0 to 0.3 mM for 30 h. (A) Cell survival was measured by using Cell Counting Kit-8. (B) PC12 cells were stained with DAPI. a, 0 mM; b, 0.1 mM; c, 0.2 mM; d, 0.3 mM. Scale bar is 50 μM. Arrows indicate the fragmented nuclei. Data represent mean±SD from three independent experiments. **p< 0.01, ***p<0.001.

Data analysis

The data are represented as the mean±SD from three independent experiments and analyzed by one-way analysis of variance (ANOVA), followed by Tukey's multiple comparison test. Differences between groups were considered statistically significant if the p values were less than 0.05.

RESULTS

$FeCl_2$ treatment decreases cell survival in PC12 cells

Cell survival and DAPI staining were examined in PC12 cells treated with $FeCl_2$ for 30 h. Cell survival in PC12 cells was significantly decreased in cells treated with 0.05, 0.10, 0.15, 0.2, 0.25, and 0.3 mM $FeCl_2$ ($p<0.01$), while that in 0.6 mM $FeCl_2$ was significantly reduced by about 75% ($p<0.001$) (Fig. 1A). This result suggests that the iron concentrations from 0.05 mM to 0.3 mM induced oxidative stress. DAPI staining with enhanced fluorescence was observed in treatment groups of 0.1, 0.2, and 0.3 mM $FeCl_2$, and the nuclei appeared fragmented in 0.2 and 0.3 mM $FeCl_2$ (Fig. 1B).

APP-α-CTF and APP-β-CTF expressions with $FeCl_2$ treatment

To investigate APP-α-CTF and APP-β-CTF expressions with $FeCl_2$ treatment, Western blot analysis was carried out, and the expression levels of *ADAM10* and *BACE1* mRNA were determined. Expressions of APP-α-CTF and APP-β-CTF were respectively increased according to $FeCl_2$ concentration ($p<0.001$) (Fig. 2). In these conditions, the

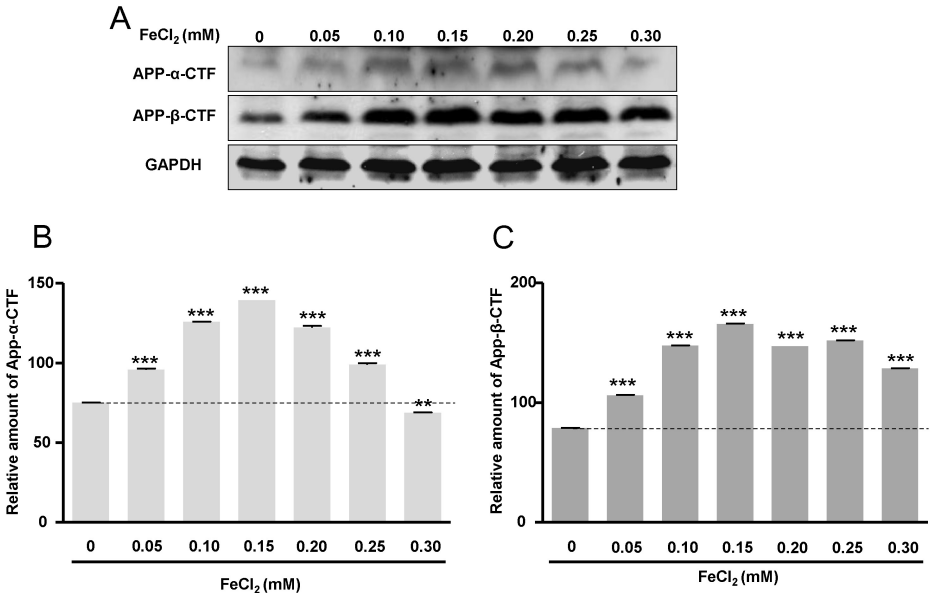

Fig. 2. Increased expression of APP-α-CTF and APP-β-CTF under $FeCl_2$ treatment in PC12 cells. (A) Western blot analysis was carried out. (B) The expression of APP-α-CTF protein was increased. (C) The expression of APP-β-CTF was evaluated. Expression of APP-α-CTF was normalized by GAPDH expression as an internal control (C). PC12 cells were incubated in DMEM containing 10% FBS and increasing concentrations of $FeCl_2$ from 0 to 0.3 mM for 30 h. Data represent mean±SD from three independent experiments. **p<0.01, ***p <0.001.

expressions of *ADAM10* and *BACE1* mRNA were increased significantly relative to the expressions of APP-α-CTF and APP-β-CTF (Fig. 3). This result indicates that increased mRNA of *ADAM10* and *BACE1* may be associated with the increases of APP-α-CTF and APP-β-CTF expression.

ERK pathway are activated by $FeCl_2$ treatment

The phosphorylation of Bad at two functional sites, S112 and S155, was investigated. The phosphorylation of Bad at S112 and S155 was increased in response to $FeCl_2$ concentration (Fig. 4A~C), and phosphorylation of Bad at S136 was slightly augmented (Fig. 4A, Fig. 4D). This indicates that the translocation of Bad was blocked from cytosol to mitochondria. Thus, mitochondrial cytochrome c release was limited [16]. In this condition, p-ERK was significantly increased (Fig. 5). Therefore, PC12 cells treated with $FeCl_2$ were associated with ERK signal pathway.

Expressions of Bcl-2 and Bax protein are related to oxidative stress

Bcl-2 protein expression was increased according to $FeCl_2$ concentration (Fig. 6A, B), but Bax protein expression was only slightly changed (Fig. 6A, C). This data was consistent with Fig. 1, suggesting that the expressions of Bcl-2 and Bax protein may be related to oxidative stress.

DISCUSSION

High concentrations of reactive iron increase oxidative-stress induced neuronal vulnerability, and iron accumulation increases the toxicity in the brain [8,9]. Cellular iron mismanagement may cause or exacerbate AD through a variety of cellular mechanisms [8,12]. Iron has been

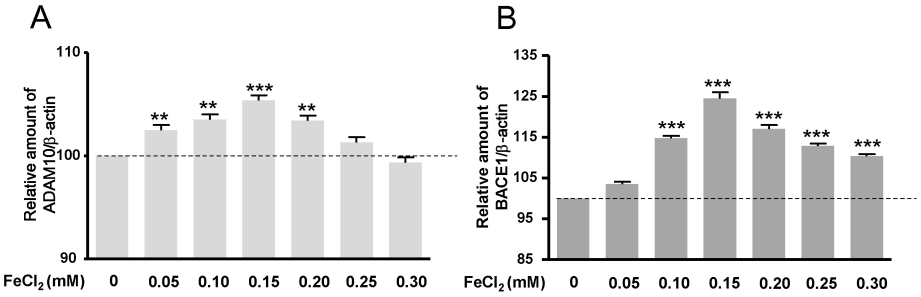

Fig. 3. Increased expression of *ADA- M10* and *BACE1* mRNA expression under $FeCl_2$ treatment in PC12 cells. Changes in *ADAM10* and *BACE1* were evaluated by quantitative real-time PCR. Expression of *ADAM10* (A) and *BACE1* (B) were normalized to *β-actin* expression as an internal control. PC12 cells were incubated in DMEM containing 10% FBS and increasing concentrations of $FeCl_2$ from 0 to 0.3 mM for 30 h. Data represent mean±SD from three independent experiments. **p<0.01, ***p<0.001.

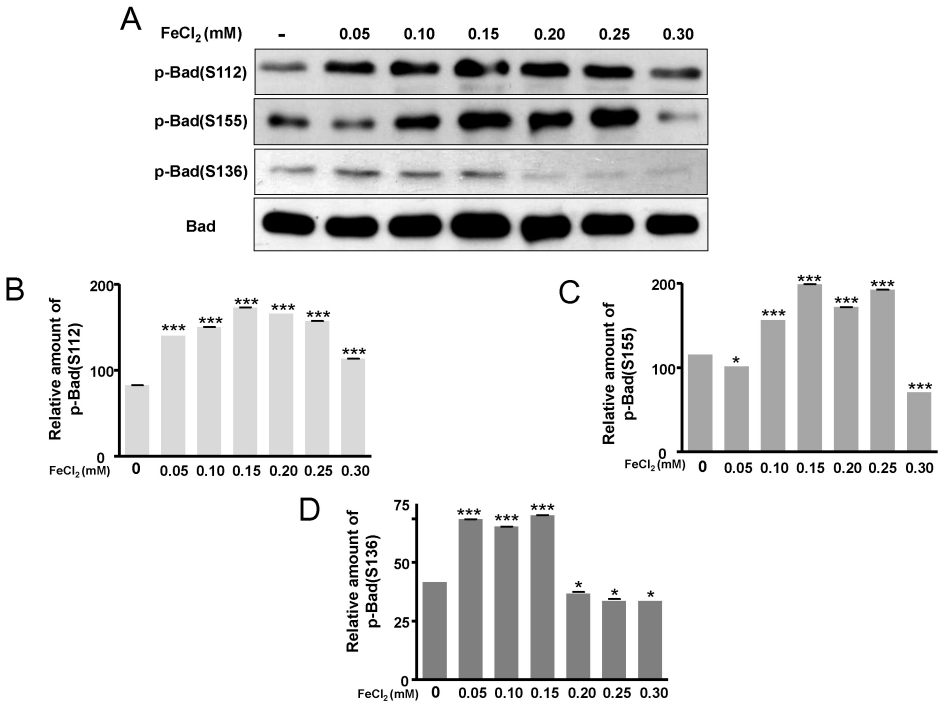

Fig. 4. Phosphorylation of Bad at S112, S155, and S136. (A) Phosphorylated forms of Bad at functional sites S112, S155, and S136 were evaluated by Western blot analysis. (B) Relative amounts of p-Bad (S112), (C) relative amount of p-Bad (S155), and (D) relative amount of p-Bad (S136) were normalized to Bad exp- ression as an internal control. PC12 cells were incubated in DMEM containing 10% FBS and increasing concentrations of $FeCl_2$ from 0 to 0.3 mM for 30 h. Data represent mean±SD from three independent experiments. *p<0.05, ***p<0.001.

shown to regulate APP synthesis and processing [8,12,13]. In this study, we have shown that iron provokes oxidative stress responses in rat PC12 cells. *BACE1* transcription levels increased at the subtoxic concentration of iron that had little effect on cell survival. Transcriptional and translational upregulation of *BACE1* can be triggered by oxidative stress [22]. *BACE1* knock-out mice fail to produce Aβ [25], indicating that BACE1 is the major enzyme for Aβ production. *BACE1* overexpression leads to the production of Aβ *in vitro* [26]. It has been reported that iron can accelerate the production of Aβ and is found in high concentrations in the amyloid plaque [7]. Therefore, oxidative stress has been considered to have a key pathogenic role in AD [27,28]. However, in the initial stages of AD, Aβ may have neuroprotective effects. Because Aβ possesses iron chelating sites, oxidative stress-induced intracellular iron levels stimulate APP holo-protein expression and the subsequent generation of Aβ as a compensatory response that eventually reduces oxidative stress [29]. This finding indicates that oxidative stress not only causes damage to cellular structures, but also provokes cellular responses. Thus, the physiological pathway of Aβ production may be considered a compensatory or neuroprotective response that reduces oxidative stress damage. These findings also support roles for Aβ in physiological iron regulation [30,31].

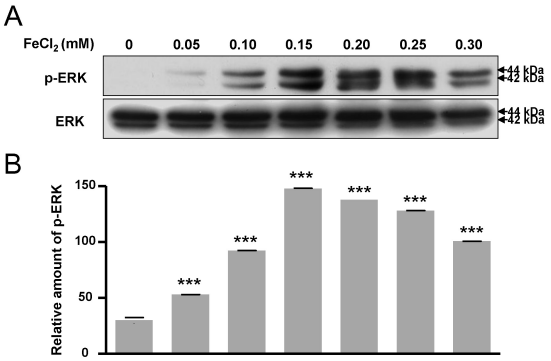

Fig. 5. Activation of ERK signal pathway. Changes in phosphorylated forms of ERK as well as ERK were evaluated by Western blot analysis (A). Expression of p-ERK was normalized to ERK expression as an internal control (B). PC12 cells were incubated in DMEM containing 10% FBS and increasing concentrations of $FeCl_2$ from 0 to 0.3 mM for 30 h. Data represent mean±SD from three independent experiments. ***p<0.001.

We show that ADAM10 is upregulated (under 0.2 mM of $FeCl_2$) and is thought to maintain physiological homeostasis in response to Aβ increase. Production of Aβ is prevented by α-secretase activity which cleaves APP in the Aβ region thereby releasing the soluble N-terminal fragment sAPPα and a C-terminal fragment that is further cleaved by γ-secretase [3]. sAPPα has been shown to exert neurotrophic and neuroprotective effects *in vitro* [32,33]. However, *ADAM10* transcription levels have no remarkable changes when treated with 0.2 mM $FeCl_2$. Apparent discrepancies between our values and those of earlier studies may be due to the effects of Aβ. Aβ may have a decisive role in reducing oxidative stress by chelating ferrous ions. Thus, we suggest that Aβ has a neuroprotective effect on transient oxidative stress or early stage AD.

Our results indicate that ERK activation protects against apoptotic cell death. It has been reported that prolonged ERK activation is accompanied by the proapoptotic effect of ERK [17], whereas a transient activation of ERK protects cells from death [18]. In the present study, we found that activation of the ERK pathway is neuroprotective at subtoxic concentrations. Thus, the protection strategies that target these mechanisms merit further exploration. Furthermore, the kinetics and duration of ERK activation may play an important role in influencing its effect on cell fate.

Bcl-2 plays a protective role against oxidative stress induced by $FeCl_2$ in rat PC12 cells. Bcl-2 is an antiapoptotic protein which reduces cytochrome c release [19]. Bax is a proapoptotic protein which induces cytochrome c release [21]. Overall, cell responses tended to reduce the release

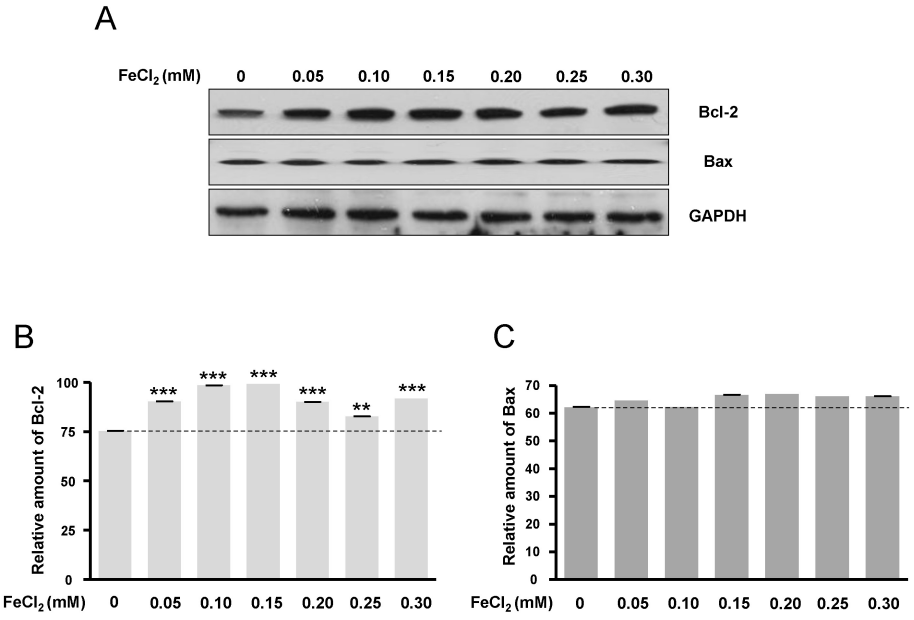

Fig. 6. Expression of Bcl-2 and Bax. (A) Proteins were measured by Western blot anaysis. (B) Relative amount of Bcl-2 and (C) relative amount of Bax. Expressions of Bcl-2 and Bax were normalized to GAPDH expression as an internal control. PC12 cells were incubated in DMEM containing 10% FBS and increasing concentrations of $FeCl_2$ from 0 to 0.3 mM for 30 h. Data represent mean±SD from three independent experiments. **p<0.01, ***p<0.001.

of cytochrome c from mitochondria. Thus, the antiapoptotic pathway is predominant. Consistent with this, the ERK pathway is activated. Phosphorylation of Bad at S112 and S155 is upregulated and implies that the antiapoptotic cell response is increased. ERK has been shown to be required for the prevention of apoptosis and the promotion of cell survival through the phosphorylation of proapoptotic Bad [34].

In conclusion, mRNA expressions of *ADAM10* and *BACE1* were associated with increases of APP-α-CTF and APP-β-CTF expression, respectively, under ferrous iron-induced oxidative stress. This process may involve p-ERK activation.

ACKNOWLEDGEMENTS

This research was supported by Basic Science Research program through the National Research Foundation of Korea (NRF) funded by the Ministry of Education, Science and technology (2010-0023849, 2012-0006787).

REFERENCES

1. **Hardy J, Selkoe DJ**. The amyloid hypothesis of Alzheimer's disease: progress and problems on the road to therapeutics. *Science*. 2002;297:353-356.
2. **Mattson MP**. Pathways towards and away from Alzheimer's disease. *Nature*. 2004;430:631-639.
3. **Pietrzik C, Behl C**. Concepts for the treatment of Alzheimer's disease: molecular mechanisms and clinical application. *Int J Exp Pathol*. 2005;86:173-185.
4. **Praticò D**. Evidence of oxidative stress in Alzheimer's disease brain and antioxidant therapy: lights and shadows. *Ann N Y Acad Sci*. 2008;1147:70-78.
5. **Maynard CJ, Cappai R, Volitakis I, Cherny RA, White AR, Beyreuther K, Masters CL, Bush AI, Li QX**. Overexpression of Alzheimer's disease amyloid-beta opposes the age-dependent elevations of brain copper and iron. *J Biol Chem*. 2002;277:44670-44676.
6. **Pallàs M, Camins A**. Molecular and biochemical features in Alzheimer's disease. *Curr Pharm Des*. 2006;12:4389-4408.
7. **Lovell MA, Robertson JD, Teesdale WJ, Campbell JL, Markesbery WR**. Copper, iron and zinc in Alzheimer's disease senile plaques. *J Neurol Sci*. 1998;158:47-52.
8. **Zecca L, Youdim MB, Riederer P, Connor JR, Crichton RR**. Iron, brain ageing and neurodegenerative disorders. *Nat Rev Neurosci*. 2004;5:863-873.
9. **Honda K, Smith MA, Zhu X, Baus D, Merrick WC, Tartakoff AM, Hattier T, Harris PL, Siedlak SL, Fujioka H, Liu Q, Moreira PI, Miller FP, Nunomura A, Shimohama S, Perry G**. Ribosomal RNA in Alzheimer disease is oxidized by bound redox-active iron. *J Biol Chem*. 2005;280:20978-20986.
10. **Hallgren B, Sourander P**. The effect of age on the non-haemin iron in the human brain. *J Neurochem*. 1958;3:41-51.
11. **Bartzokis G, Beckson M, Hance DB, Marx P, Foster JA, Marder SR**. MR evaluation of age-related increase of brain iron in young adult and older normal males. *Magn Reson Imaging*. 1997;15:29-35.
12. **Bartzokis G**. Age-related myelin breakdown: a developmental model of cognitive decline and Alzheimer's disease. *Neurobiol Aging*. 2004;25:5-18.
13. **Bartzokis G, Tishler TA, Lu PH, Villablanca P, Altshuler LL, Carter M, Huang D, Edwards N, Mintz J**. Brain ferritin iron may influence age-and gender-related risks of neurodegeneration. *Neurobiol Aging*. 2007;28:414-423.
14. **Zhu X, Castellani RJ, Takeda A, Nunomura A, Atwood CS, Perry G, Smith MA**. Differential activation of neuronal ERK, JNK/SAPK and p38 in Alzheimer disease: the 'two hit' hypothesis. *Mech Ageing Dev*. 2001;123:39-46.
15. **Li G, Yang Q, Krishnan S, Alexander EA, Borkan SC, Schwartz JH**. A novel cellular survival factor--the B2 subunit of vacuolar H^+-ATPase inhibits apoptosis. *Cell Death Differ*. 2006;13:2109-2117.
16. **Kennedy SG, Kandel ES, Cross TK, Hay N**. Akt/Protein kinase B inhibits cell death by preventing the release of cytochrome c from mitochondria. *Mol Cell Biol*. 1999;19:5800-5810.
17. **di Mari JF, Davis R, Safirstein RL**. MAPK activation determines renal epithelial cell survival during oxidative injury. *Am J Physiol*. 1999;277:F195-203.
18. **Arany I, Megyesi JK, Kaneto H, Tanaka S, Safirstein RL**. Activation of ERK or inhibition of JNK ameliorates H(2)O(2) cytotoxicity in mouse renal proximal tubule cells. *Kidney Int*. 2004;65:1231-1239.
19. **Gottlieb RA**. Role of mitochondria in apoptosis. *Crit Rev Eukaryot Gene Expr*. 2000;10:231-239.
20. **Howard S, Bottino C, Brooke S, Cheng E, Giffard RG, Sapolsky R**. Neuroprotective effects of bcl-2 overexpression in hippocampal cultures: interactions with pathways of oxidative damage. *J Neurochem*. 2002;83:914-923.
21. **Starkov AA, Polster BM, Fiskum G**. Regulation of hydrogen peroxide production by brain mitochondria by calcium and Bax. *J Neurochem*. 2002;83:220-228.
22. **Zacchetti D, Chieregatti E, Bettegazzi B, Mihailovich M, Sousa VL, Grohovaz F, Meldolesi J**. BACE1 expression and activity: relevance in Alzheimer's disease. *Neurodegener Dis*. 2007;4:117-126.
23. **Mohajeri MH, Saini KD, Nitsch RM**. Transgenic BACE expression in mouse neurons accelerates amyloid plaque pathology. *J Neural Transm*. 2004;111:413-425.
24. **Nakamura M, Shishido N, Nunomura A, Smith MA, Perry G, Hayashi Y, Nakayama K, Hayashi T**. Three histidine residues of amyloid-beta peptide control the redox activity of copper and iron. *Biochemistry*. 2007;46:12737-12743.
25. **Roberds SL, Anderson J, Basi G, Bienkowski MJ, Branstetter DG, Chen KS, Freedman SB, Frigon NL, Games D, Hu K, Johnson-Wood K, Kappenman KE, Kawabe TT, Kola I, Kuehn R, Lee M, Liu W, Motter R, Nichols NF, Power M, Robertson DW, Schenk D, Schoor M, Shopp GM, Shuck ME, Sinha S, Svensson KA, Tatsuno G, Tintrup H, Wijsman J, Wright S, McConlogue L**. BACE knockout mice are healthy despite lacking the primary beta-secretase activity in brain: implications for Alzheimer's disease therapeutics. *Hum Mol Genet*. 2001;10:1317-1324.
26. **Lee EB, Skovronsky DM, Abtahian F, Doms RW, Lee VM**. Secretion and intracellular generation of truncated Abeta in beta-site amyloid-beta precursor protein-cleaving enzyme expressing human neurons. *J Biol Chem*. 2003;278:4458-4466.
27. **Cross CE, Halliwell B, Borish ET, Pryor WA, Ames BN, Saul RL, McCord JM, Harman D**. Oxygen radicals and human disease. *Ann Intern Med*. 1987;107:526-545.
28. **Smith MA, Sayre LM, Monnier VM, Perry G**. Radical AGEing in Alzheimer's disease. *Trends Neurosci*. 1995;18:172-176.
29. **Avramovich-Tirosh Y, Amit T, Bar-Am O, Weinreb O, Youdim MB**. Physiological and pathological aspects of Abeta in iron homeostasis via 5'UTR in the APP mRNA and the therapeutic use of iron-chelators. *BMC Neurosci*. 2008;9 Suppl 2:S2.
30. **Smith MA, Nunomura A, Zhu X, Takeda A, Perry G**. Metabolic, metallic, and mitotic sources of oxidative stress in Alzheimer disease. *Antioxid Redox Signal*. 2000;2:413-420.
31. **Atwood CS, Obrenovich ME, Liu T, Chan H, Perry G, Smith MA, Martins RN**. Amyloid-beta: a chameleon walking in two worlds: a review of the trophic and toxic properties of amyloid-beta. *Brain Res Brain Res Rev*. 2003;43:1-16.
32. **Mattson MP, Cheng B, Culwell AR, Esch FS, Lieberburg I, Rydel RE**. Evidence for excitoprotective and intraneuronal calcium-regulating roles for secreted forms of the beta-amyloid precursor protein. *Neuron*. 1993;10:243-254.
33. **Furukawa K, Sopher BL, Rydel RE, Begley JG, Pham DG, Martin GM, Fox M, Mattson MP**. Increased activity-regulating

and neuroprotective efficacy of alpha-secretase-derived secreted amyloid precursor protein conferred by a C-terminal heparin-binding domain. *J Neurochem*. 1996;67:1882-1896.

34. **Kim JY, Kim YJ, Lee S, Park JH**. The critical role of ERK in death resistance and invasiveness of hypoxia-selected glioblastoma cells. *BMC Cancer*. 2009;9:27.